Modelling of fibre pull-out from a cement matrix

Youjiang Wang, Victor C. Li† and Stanley Backer**

Synopsis Theoretical analyses of fibre pull-out from a matrix reported in the literature are briefly reviewed. The effects of Poisson's ratio, elastic–frictional bond strengths, and bond strength variation with slippage distance on the pull-out relation are discussed. A theoretical model motivated by observations of fibre surface abrasion is developed to predict the pull-out force versus displacement relationship. The model takes into consideration the variation of the frictional fibre–matrix bond strength with fibre slippage distance. Good agreement is achieved between model predicted pull-out behaviour and experimental pull-out curves for nylon and polypropylene fibres. For these synthetic fibres, the bond strength increases with the slippage distance during the process of pull-out. The model also predicts reasonably well the pull-out behaviour of steel fibres for which the bond strength decreases with the slippage distance.

Keywords Mathematical model, fibre reinforced concrete, bonding strength, portland cements, nylon fibres, polypropylene fibres, metal fibres, pull-out tests, fibre cement composites, fibre–matrix bond, bond stress, shear strength, frictional bond.

INTRODUCTION

Fibre pull-out tests are often used to study the fibre–matrix bond behaviour in fibre reinforced cement composites (FRC), a factor strongly influencing the properties of the composites. The pull-out test is also important by itself as it simulates the fibre bridging–pull-out phenomenon during the fracture process of FRC. In relating the pull-out test results with the fibre–matrix bond characteristics, numerous models have been developed and many of them have been reviewed [1, 2]. A uniform shear bond strength between the fibre and the matrix is often assumed in FRC models [3, 4] and the bond strength from pull-out tests is frequently reported in terms of the average value over the embedded fibre surface area [1, 5, 6]. Obviously, the uniform shear stress does not necessarily represent the actual stress state at the fibre–matrix interface.

When a load is applied to pull a fibre out from a cement matrix, triaxial stress state generally exists at the fibre–matrix interface, primarily due to the radial contraction of the fibre. The effect of fibre radial contraction (Poisson's effect) during pull-out was discussed by Kelly and Zweben [7], Pinchin [8], and Baggott and Gandhi [9]. Their analyses show theoretically that for certain types of fibres (e.g. polypropylene), the pull-out process will involve unstable debonding and concrete reinforced with these fibres aligned in the matrix will not exhibit multiple cracking due to their unfavourable Poisson's ratios. However, the experimental results of Baggott and Gandhi [9] indicated that slight misalignment in the specimen and the asperities of the fibre surface could offset the Poisson's effect. Multiple cracking of FRC reinforced with aligned polypropylene fibres was observed in their direct tension test, which was not expected according to the theories for perfect fibre alignment and smooth fibre surface. Since slight misalignment in pull-out test is unavoidable and no unstable load drop has been observed even in the authors' pull-out tests of nylon and polypropylene fibres which have relatively high Poisson's ratios [10], it follows that in general the Poisson's effect can be neglected in fibre pull-out analysis and that a one dimensional model is usually adequate to describe the fibre pull-out test.

Lawrence [11] and Gopalaratnam and Shah [12] have obtained one dimensional solutions to the fibre pull-out problem in which gradual debonding of the elastic bond was considered (Figure 1). In both models, a perfect elastic bond between the fibre and the matrix is first assumed and the elastic shear stress field is obtained. Debonding takes place when the maximum shear stress reaches the elastic bond strength, τ_s. The shear stress in the debonded region is determined by the frictional bond strength, τ_i. Both τ_s and τ_i are assumed to be constant during the pull-out process. Because of the inadequately defined geometry in Lawrence's model which uses some parameters to lump the effect of geometry and material properties, the use of this model

* Department of Mechanical Engineering and † Department of Civil Engineering, Massachusetts Institute of Technology, Cambridge, MA 02139

Received 25 January 1988 Accepted 20 April 1988

0262-5075/88/10301143/$02.00

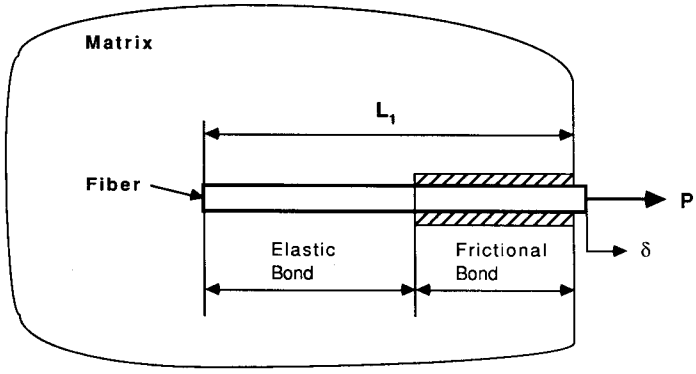

Figure 1 Schematic illustration of a partially debonded fibre during pull-out

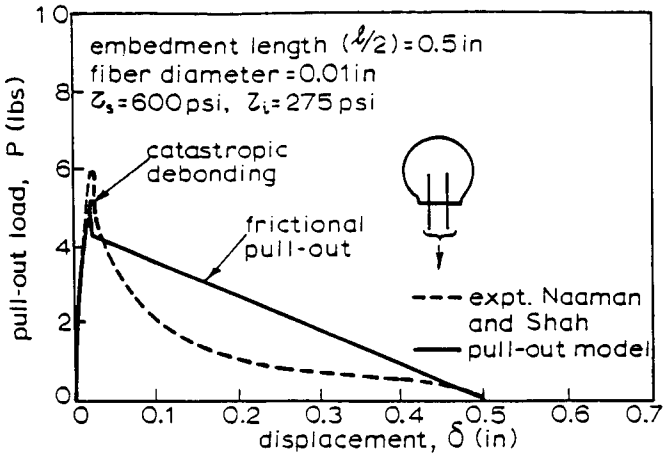

Figure 2 Comparison of the pull-out load displacement behaviour predicted by Gopalaratnam and Shah's model [12] with experimental results by Naaman and Shah [13] (1 lb = 4.45 N, 1 in. = 25.4 mm, 1 psi = 0.0069 MPa; After Gopalaratnam and Shah [12])

is very limited [1]. The model by Gopalaratnum and Shah has been used to predict the result of steel fibre pull-out test [12] (Figure 2).

It has been shown [11, 12] that both τ_s and τ_i are important parameters to characterise the debonding process of fibre pull-out and to determine the conditions for unstable debonding. However, the effect of the elastic bond strength, τ_s, on the overall pull-out response is not always significant. During debonding, the shear stress intensity in the elastically bonded region decays approximately exponentially with the distance from the debonding point, with a maximum stress equal to τ_s. The length of the fibre segment strongly influenced by this elastic stress field (the length over which the shear stress is not near zero) is dependent on, among other quantities, the ratio between fibre modulus (E_f) and the matrix modulus (E_m), and the fibre cross-sectional area. For low modulus fibres, or even high modulus fibres with high aspect ratio (length to diameter ratio), the elastic stress field has relatively little effect on the pull-out load-displacement relation except at the very early stage of debonding. Figure 3 shows a calculation example in which the load-displacement curves for both $\tau_s = 2\tau_i$ and $\tau_s = 0$ are compared for cases with $E_f/E_m = 10$ but with different fibre lengths, based on the theoretical relations derived by Gopalaratnam and Shah [12]. As shown by this specific example, there is no noticeable effect of the elastic bond strength (τ_s) on the pull-out load-displacement relations for embedded length $L_1 = 20$ mm, and some, but not significant effect for $L_1 = 5$ mm. From Figure 3(a), it appears that the inclusion of the elastic shear stress field in the calculation would result in an initially less stiff P–δ response than for $\tau_s = 0$. This could be caused by neglecting the matrix deformation in the calculation of fibre pull-out displacement [12]. Presumably the matrix deformation is more localised and larger near the exit end of the fibre for the case of bonded fibre, and more uniform along the fibre length for the case of purely frictional resistance. If the P–δ curves in Figure 3(a) were corrected for the matrix deformation, the discrepancy in the stiffness of these curves noted earlier could be expected to disappear. It can be shown that for lower E_f/E_m ratio or higher fibre aspect ratio, the τ_s effect is even less. Notice further that the displacement before complete debonding corresponds only to a minute fraction of the total pull-out displacement. After complete debonding, the elastic bond strength has no consequent effect. Therefore in most cases the pull-out analysis can be simplified by neglecting the elastic stress field.

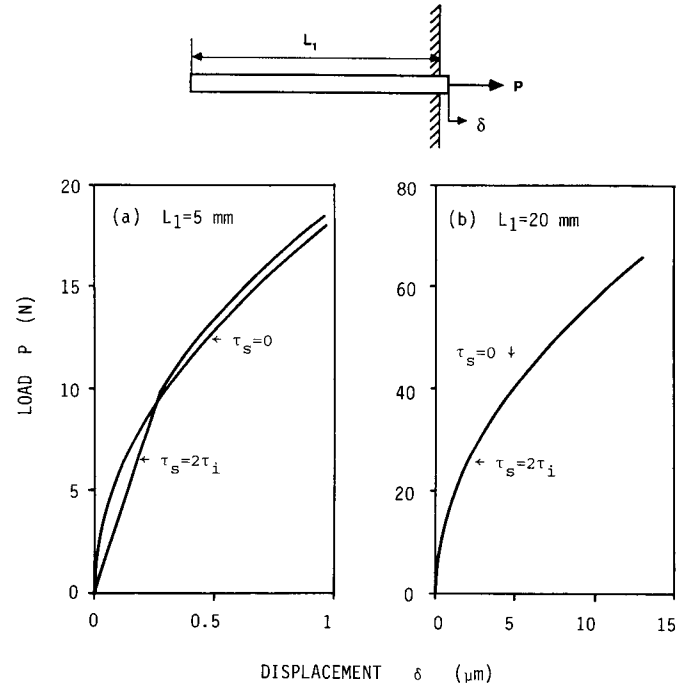

Figure 3 Effect of the elastic bond strength τ_s on the theoretical load displacement response before complete debonding: (a) $L_1 = 5$ mm, (b) $L_1 = 20$ mm ($\tau_i = 2$ MPa, fibre diameter $d_f = 0.5$ mm, $E_f = 270$ GPa, $E_m = 27$ GPa, matrix shear modulus $G_m = 11.3$ GPa, matrix cross-sectional area $A_m = 200\,mm^2$)

The frictional bond strength (τ_i) in general varies with the slippage distance (s) between the fibre and the matrix during the process of pull-out. The effect of the variation of τ_i with s has been discussed by the authors [10]. In steel fibre pull-out, τ_i often decreases with s as a result of the breakdown of the cement at the fibre–matrix interface due to the stiffness and hardness of the steel fibre. The decrease in τ_i during steel fibre pull-out is responsible for the significant discrepancy between the experimental curve and theoretical result by Gopalaratnam and Shah using a constant τ_i, as seen in the descending part in Figure 2. In synthetic fibre pull-out test with nylon and polypropyelene fibres, τ_i was found to increase with s due to fibre surface abrasion and accumulation of wear debries [10]. Clearly, it is highly inaccurate to simply use a constant frictional bond strength to describe the fibre pull-out process after complete debonding of the elastic bond. In this paper, a theoretical model is developed which takes into consideration the variation of the frictional bond strength during pull-out. The primary objective of this study is to understand the behaviour of a fibre in an FRC member during fracture. With additional considerations of fibre orientation and fibre distribution, the results of this study can contribute to the prediction of FRC constitutive relations.

THEORETICAL MODELLING

Basic assumptions

Among the many configurations often used for the pull-out test, the pull-out of a fibre embedded across a matrix crack, illustrated in Figure 4, is of particular interest because of its similarity to the fibre bridging situation in FRC fracture process. To predict the pull-out load vs. crack separation relation for this 'two-sided pull-out' problem, a few simplifying assumptions are first made. The fibre is assumed to be linear elastic and sufficiently strong to enable complete pull-out without rupture. The contribution of matrix deformation to the crack separation is neglected. Based on the above discussion, both the Poisson's effect and the elastic bond strength are neglected in this analysis. The distinctive feature of this model lies in its assumption that the fibre–matrix frictional bond strength (denoted as τ afterwards) for an infinitesimal fibre segment is a function of its slippage distance (s) with respect to the matrix, described by a τ–s law. Using such a τ–s relationship for the fractional bond strength instead of a constant value has been shown necessary in the previous section.

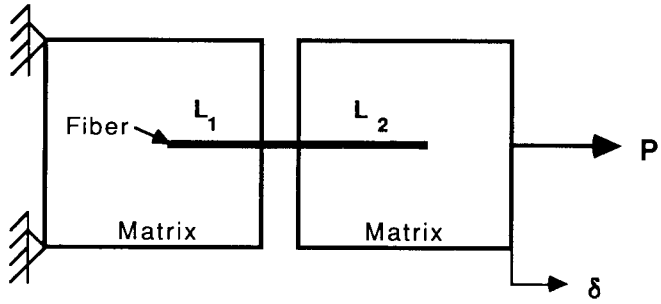

Figure 4 Schematic illustration of a pull-out specimen configuration

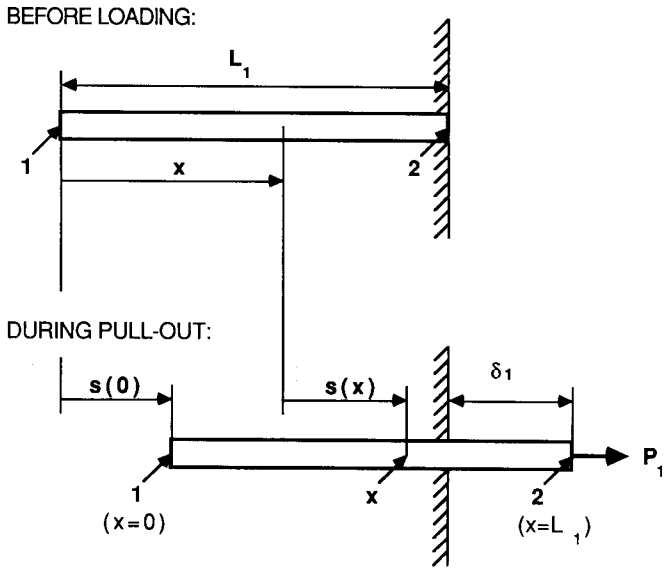

Figure 5 Illustration of direct fibre pull-out problem

The direct pull-out problem

Before solving the two-sided pull-out problem, the direct pull-out (one-sided) of an embedded fibre from a cement matrix, shown in Figure 5, needs to be considered. The x coordinate system in the figure is with respect to the undeformed fibre geometry (before loading) and is associated with the material particles. For example, during the process of pull-out, x always equals 0 for Point 1, the embedded end, and equals L_1 for Point 2, the loading end.

The slippage distance, s(x), with respect to the matrix of an infinitesimal fibre segment at x is equal to the sum of the slippage distance of the fibre embedded end, s(0), plus the elastic elongation of the fibre segment located between 0 and x:

$$s(x) = s(0) + \int_0^x \epsilon(x)\, dx \qquad (1)$$

Note that s(0) = 0 before complete debonding, and s(0) varies from 0 to L_1 during subsequent pull-out. The axial strain of the fibre, $\epsilon(x)$, can simply be calculated from the fibre axial load P(x):

$$\epsilon(x) = \frac{4}{\pi d_f^2 E_f} P(x) \qquad (2)$$

and P(x) is given from the equilibrium condition:

$$P(x) = Po + \int_0^x \tau(x)\, \pi\, d_f\, [1 + \epsilon(x)]\, dx \qquad (3)$$

where P_o is a constant representing the fibre end anchorage effect when the fibre end slips (P_o = 0 before

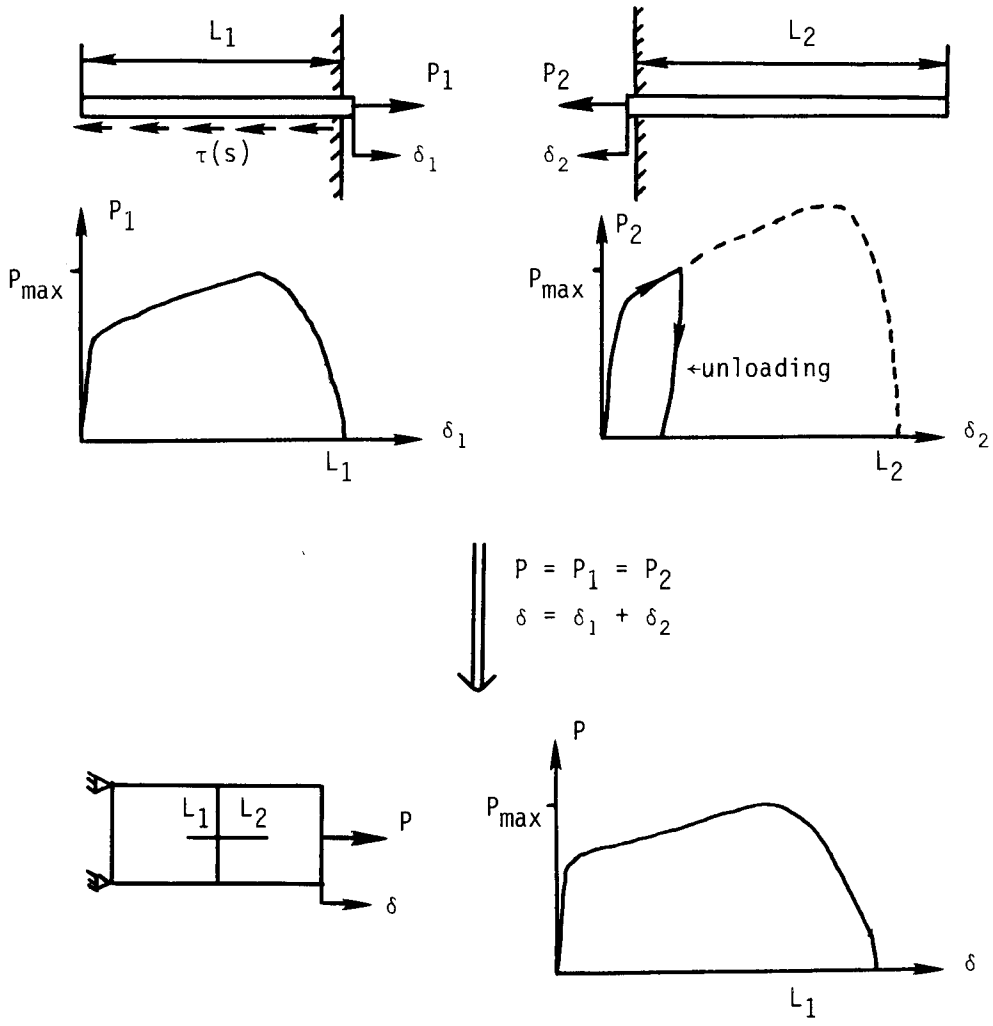

Figure 6
Illustration of calculation procedures for the two-sided pull-out problem

complete debonding). P_o usually is very small, and can be estimated from the experimental load vs. crack separation curves. The shear stress, $\tau(x)$, between the fibre and the matrix is determined by the slippage distance, $s(x)$, given by the τ–s law as $\tau(s)$, for fibre sections inside the matrix:

$$\tau(x) = \tau(s(x)) \quad \text{for } x+s(0) < L_1 \text{ (inside matrix)} \quad (4a)$$

$$\tau(x) = 0 \quad \text{for } x+s(0) \geqslant L_1 \text{ (outside matrix)} \quad (4b)$$

These equations, equation (1) to equation (4), are, in general, coupled nonlinear questions, but can be solved by numerical methods without iteration.

At each loading stage, the load and the corresponding displacement can be obtained after solving these equations from:

$$P_1 = P(x = L_1) \quad (5)$$

$$\delta_1 = s(x = L_1) \quad (6)$$

The two-sided pull-out problem

For a fibre embedded in a matrix across a crack plane, as that shown in Figure 4, the pull-out of the short and the longer fibre segments are first analysed separately, and then these load and displacement responses are combined to obtain the total load-displacement relation, as illustrated in Figure 6. Details of this procedure are described in this section.

The fibre in the matrix is not directly loaded by external forces. Instead, the load in the fibre is transferred from the fibre–matrix interface. Apparently, the longer fibre segment (L_2) would provide a higher pull-out force than the shorter segment (L_1) if they were pulled out independently. For this reason, the shorter fibre segment will be pulled out from the matrix as though it were directly pulled out by an external force, and the load-displacement relation P_1–δ_1 derived in the previous section applies to this process. Due to equilibrium constraint, the pulling forces for both segments must be equal, i.e. $P_1 = P_2$. The maximum pulling force experienced by the longer fibre segment during the two-sided pull-out will be the same as that for the shorter fibre segment.

Before reaching the maximum load P_{max}, the longer fibre segment (L_2) is monotonically loaded with pulling force provided by the shorter fibre segment (L_1), and the

longer segment deforms and slips in response to the load according to the load–displacement relationship derived for the one-sided pull-out problem (after replacing subscript '1' with '2' in equations 1–6).

The axial force, the axial strain, and the slippage distance states at $P = P_{max}$ provide the initial conditions for the unloading process. Referring to Figure 7a, the axial force, strain, and slippage distance as functions of coordinate x at the instant of $P = P_{max}$ are designated as $P_m(x)$, $\epsilon_m(x)$ and $s_m(x)$, respectively. After reaching the maximum load P_{max}, the load in the shorter segment will drop, and so will the load in the longer segment (P_2). Since the longer segment still has the potential for higher loads and the load actually decreases, the segment can no longer be pulled out and its embedded end will remain where it was when the load reached P_{max}. During unloading, part of the elastic elongation of the longer fibre segment is recovered and the fibre tends to 'shrink back' into the matrix, and this is resisted by the fibre–matrix interfacial frictional stress. For a given unloading instant, a parameter h is defined to be the x-coordinate at which the shear stress reverses its direction as shown in Figure 7b. The fibre section with $x \leqslant h$ is not affected by unloading. For $x \leqslant h$, the axial force, strain, and slippage distance associated with P_{max} are maintained at $P_m(x)$, $\epsilon_m(x)$, and $s_m(x)$, i.e.

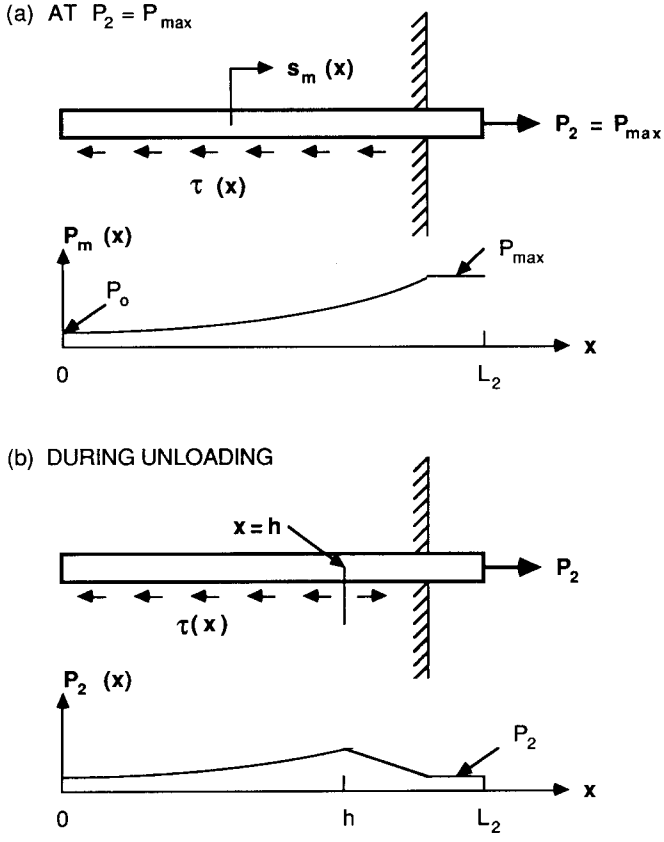

Figure 7 Schematic diagram for determination of load displacement relation at P_{max} and during unloading for the longer fibre segment (L_2)

$$P(x) = P_m(x) \qquad (x \leqslant h) \qquad (7)$$

$$\epsilon(x) = \epsilon_m(x) \qquad (x \leqslant h) \qquad (8)$$

$$s(x) = s_m(x) \qquad (x \leqslant h) \qquad (9)$$

Beyond h (i.e. for $x > h$), the load is found from equilibrium conditions as:

$$P(x) = P_m(h) - \int_h^x \tau(x)\,\pi\,d_f\,[1 + \epsilon(x)]\,dx \quad (x > h) \qquad (10)$$

and the slippage distance at x is given by the slippage distance when $P = P_{max}$ ($s_m(x)$) plus the sliding distance due to fibre elastic shrinkage:

$$s(x) = s_m(x) + \int_h^x [\epsilon_m(h) - \epsilon(x)]\,dx \quad (x > h) \qquad (11)$$

Similar to equation (4), the shear stress distribution is given by:

$$\tau(x) = \tau\,(s(x)) \quad \text{for } x + s\,(0) < L_2 \text{ (inside matrix)} \qquad (12a)$$

$$\tau(x) = 0 \quad \text{for } x + s\,(0) \geqslant L_2 \text{ (outside matrix)} \qquad (12b)$$

and the relationship between the axial force (P(x)) and the axial strain ($\epsilon(x)$) is the same as equation (2). Once these equations are solved, the pull-out load and the displacement corresponding to the instant in the unloading process can be obtained from:

$$P_2 = P(x = L_2) \qquad (13)$$

$$\delta_2 = s(x = L_2) \qquad (14)$$

By decreasing h from L_2 (no unloading when $P_2 = P_{max}$) until $P_2 = 0$, the P_2–δ_2 relationship for the unloading process can be obtained.

To calculate the complete load–displacement (crack separation) relationship, first the P_1–δ_1 curve for the shorter fibre segment is computed, from which the maximum load P_{max} is identified. Then the loading and unloading parts of the P_2–δ_2 curve for the longer fibre segment are calculated. Finally, by adding the displacements of both segments together ($\delta = \delta_1 + \delta_2$) for the corresponding load ($P = P_1 = P_2$), the complete load vs. crack separation curve, P–δ, is obtained. This procedure has been illustrated schematically in Figure 6. Note that the function δ(P) is multivalued, therefore this operation must be performed on the branches before and after P reaches P_{max} separately.

Theoretical predictions

Theoretical load vs. crack separation curves for the pull-out tests were calculated based on the model. The τ(s) functional relationship used in the model can be expressed in any convenient form, such as linear, multilinear, piecewise constant, or polynomial. In the calculations, the frictional bond strength (τ) was assumed to be a quadratic function of the slippage distance (s):

$$\tau(s) = a_0 + a_1\,s + a_2\,s^2 \qquad (15)$$

where a_0, a_1, and a_2 are constants, determined empirically such that the theoretical curves are reasonably close to the experimental results.

The theoretical predictions for nylon and polypropylene fibre pull-out are shown in Figure 8 and the experimental results are given in Figure 9. In these tests, the specimen configuration shown in Figure 4 was used, with d_f = 0.508mm, L_1 = 50mm, and L_2 = 70mm, for both nylon and polypropylene. Cement paste matrix was used and the specimen age at test was three days. Details of the experiments have been reported elsewhere [10]. Figure 10 shows the theoretical prediction for steel fibre pull-out together with the experimental result reported by Naaman and Shah [13]. The difference between the predicted and the experimental curves in the ascending part in Figure 10 is presumably due to the inclusion of deformations other than fibre elongation (e.g. testing machine and fixture deformations) in the experimental curve, for a fibre elongation of 0.25mm (displacement near peak load in experimental curve) would correspond to a uniform fibre strain of 2%, requiring an axial load over 800N in the fibre if the steel fibre could still remain linear elastic.

By comparing the experimental load vs. crack separation curves with the theoretical results, it can be seen that the proposed model is indeed able to predict closely the pull-out test result. However, it should be pointed out that the $\tau-s$ relations determined empirically are unlikely to be fully independent of geometry and loading conditions. An alternative expression based on the theory for fibre on cement friction and wear might be more desirable to represent the $\tau-s$ relationship.

It is interesting to note from these results the strong

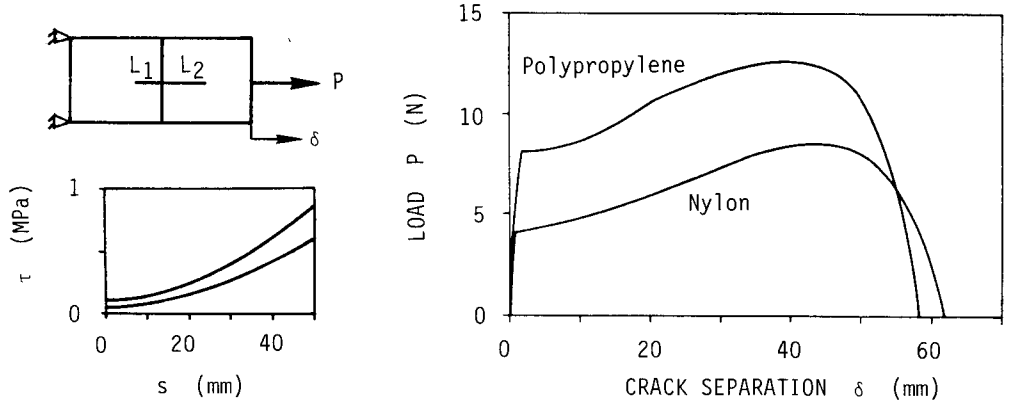

Figure 8
Theoretical predictions for nylon and polypropylene fibre pull-out. Figure on left shows the $\tau-s$ relations used. (d_f = 0.508mm, E_f = 1GPa, L_1 = 50mm, L_2 = 70mm, P_o = 0)

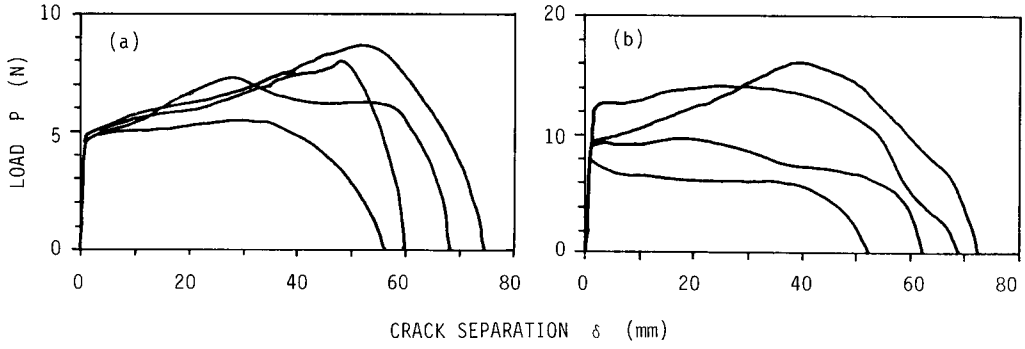

Figure 9
Experimental results for the fibre pull-out tests: (a) Nylon fibre, (b) Polypropylene fibre

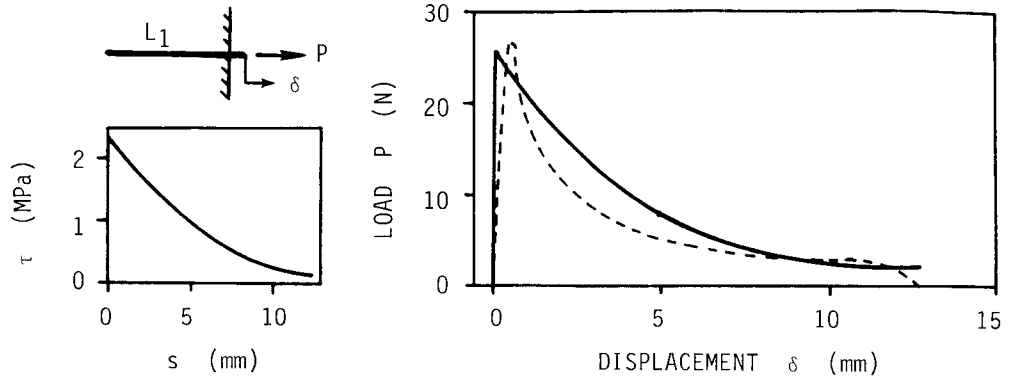

Figure 10
Comparison of model prediction (solid line) with experimental result (broken line) by Naaman and Shah [13] for steel fibre pull-out test. Figure on left shows the $\tau-s$ relation used. (d_f = 0.254mm, E_f = 209GPa, L_1 = 12.7mm, P_o = 2N)

influence of the $\tau - s$ relation on fibre pull-out response. In the case when τ increases with s due to fibre surface abrasion as seen in synthetic fibres like nylon and polypropylene, the pull-out load could remain at relatively high level over a wide range of crack separation, and the final crack separation could be greater than the embedded length of the shorter fibre segment. These contribute to an increase in energy absorption during pull-out and could have important implications on the crack resistance of FRC [14].

CONCLUSIONS

Fibre pull-out is often modelled with an elastic bond strength and a frictional bond strength for the fibre–matrix interface. However, the frictional bond strength generally varies with the fibre slippage distance relative to the matrix. In this study, a theoretical model for the pull-out test has been developed which takes into account the bond strength variation during pull-out. Good predictions of the experimental load vs. crack separation relations are obtained for pull-out tests with nylon, polypropylene as well as steel fibres.

ACKNOWLEDGEMENTS

The authors would like to acknowledge the support of the Shimizu Construction Company, Ltd. and the Program of System Engineering for Large Structures at National Science Foundation.

REFERENCES

1. Bartos, P., 'Review paper: Bond in fibre reinforced cements and concretes', The International Journal of Cement Composites, Vol. 3, No. 3, August 1981, pp. 159–77.
2. Gopalaratnam, V. S. and Shah, S. P., 'Failure mechanisism and fracture of fibre reinforced concrete', ACI Special Publication SP–105 Fibre Reinforced Concrete: Properties and Applications, American Concrete Institute, 1987, pp. 1–25.
3. Aveston, J., Cooper, G. A. and Kelly, A., 'Single and multiple fracture', in: The Properties of Fibre Composites, Conference Proceedings, National Physica Laboratory, IPC Science and Technology Press Ltd., November 1971, pp. 15–26.
4. Wang, Y., 'Mechanics of fibre reinforced concrete', S.M. Thesis, Massachusetts Institute of Technology, 1985.
5. Mindess, S. and Young, J. F., 'Concrete', Printice-Hall, Inc., Englewood Cliffs, N.J., 1981, pp. 633.
6. Wang, Y., Backer, S. and Li, V. C., 'An experimental study of synthetic fibre reinforced cementitious composites', Journal of Materials Science, Vol. 22, No. 12, December 1987, pp. 4281–91.
7. Kelly, A. and Zweben, C., 'Poisson contraction in aligned fibre composites showing pull-out', Journal of Materials Science, Vol. 11, No. 3, March 1976, pp. 582–7.
8. Pinchin, D. J., 'Poisson contraction effect in aligned fibre composities', Journal of Materials Science, Vol. 11, No. 8, August 1976, pp. 1578–81.
9. Baggott, R. and Gandhi, D., 'Multiple cracking in aligned polypropylene fibre reinforced cement composites', Journal of Materials Science, Vol. 16, No. 1, January 1981, pp. 65–74.
10. Wang, Y., Li, V. C. and Backer, S., 'Analysis of synthetic fibre pull-out from a cement matrix', in: Bonding in Cementitious Composites, Edited by S. Mindess and S. P. Shah, Material Research Society Symposium Proceedings, Vol. 114, Materials Research Society, Pittsburgh, 1988, pp. 159–65.
11. Lawrence, P., 'Some theoretical considerations of fibre pull-out from an elastic matrix', Journal of Materials Science, Vol. 7, No. 1, January 1972, pp. 10–6.
12. Gopalaratnam, V. S. and Shah, S. P., 'Tensile fracture of steel fibre reinforced concrete', ASCE Journal of Engineering Mechanics, Vol. 113, No. 5, May 1987, pp. 635–52.
13. Naaman, A. E. and Shah, S. P., 'Pull-out mechanism in steel fibre reinforced concrete', Journal of the Structural Division, American Society of Civil Engineers, Vol. 102, No. ST8, August 1976, pp. 1537–48.
14. Li, V. C., Wang, Y. and Backer, S., 'Effect of fibre-matrix bond strength on the crack resistance of synthetic fibre reinforced cementitious composities', in: Bonding in Cementitious Composites, Edited by S. Mindess and S. P. Shah, Material Research Society Symposium Proceedings, Vol. 114, Materials Research Society, Pittsbough, 1988, pp. 167–73.